Journal of Power Sources 196 (2011) 7481–7487

Contents lists available at ScienceDirect

Journal of Power Sources

journal homepage: www.elsevier.com/locate/jpowsour

Synthesis and characterization of polysulfone-containing sulfonated side chains for direct methanol fuel cells

Yuanqin Zhu, Arumugam Manthiram*

Electrochemical Energy Laboratory, Materials Science and Engineering Program, University of Texas at Austin, 1 University Station C2200, Austin, TX 78712, USA

ARTICLE INFO

Article history:
Received 29 December 2010
Received in revised form 11 May 2011
Accepted 12 May 2011
Available online 19 May 2011

Keywords:
Polysulfone
Proton exchange membranes
Direct methanol fuel cells

ABSTRACT

Two series of novel polysulfone-based ionomers containing pendant sulfonic acid groups (designated as PSf-sph-*y* and PSf-sna-*z*) have been prepared using commercially available polysulfone and sulfoaryl monomers. The synthesized ionomers have been characterized by nuclear magnetic resonance, differential scanning calorimetry, and thermogravimetric analysis. The thermal characterization data show that these polymers are stable up to 210 °C in acid form and 270 °C in salt form in air. Ion exchange capacity, water uptake, swelling, proton conductivity, and methanol permeability of the membranes have been investigated and compared with those of Nafion 115. The PSf-sna-*z* membranes bearing highly ionic groups on the flexible side chains show lower water uptake, swelling, and methanol permeability compared to the PSf-sph-*y* and Nafion 115 membranes. The optimized PSf-sna-58 membrane shows better performance in direct methanol fuel cells (DMFC) than Nafion 115 membranes.

1. Introduction

Polymer electrolyte membrane (PEM) is one of the key components of proton exchange membrane fuel cells (PEMFC) and direct methanol fuel cells (DMFC) [1,2]. PEMs should provide a fast pathway for the H^+ ions from the anode to the cathode while preventing the mixing of the fuel and oxidant gas. In the case of DMFC, the methanol permeability through the PEM from the anode to the cathode should also be low to minimize performance loss at the cathode catalyst and the waste of methanol fuel [3]. Unfortunately, the commercially available Nafion® membranes suffer from high methanol crossover from the anode to the cathode because the fluoroalkanes form wide ionic channels have high affinity for methanol, and its high cost hamper the commercialization of the DMFC technology [4]. Many approaches have been taken over the years to reduce the methanol permeation, including modified perfluorinated materials [5], sulfonated polyhydrocarbons [6], acid–base blends [7], and inorganic–organic composite materials [8].

Aromatic hydrocarbon-based polymeric electrolytes including sulfonated poly(ether ketone)s, poly(ether sulfone)s, and polyimides have been pursued as alternative membranes in recent years due to their lower methanol permeability and lower cost compared to Nafion® as well as good thermal stability [9–11]. However, most of these sulfonated membranes in which the sulfonic acid groups are incorporated directly onto the backbones generally suffer from high water swelling and poor hydrolytic stability on increasing the degree of sulfonation [12]. To improve the osmotic and hydrolytic stability of the sulfonated polymers, it is desirable to increase the hydrophilic–hydrophobic separation by locating the sulfonic acid groups away from the polymer main chains. By separating the main-chain polymer and the acidic units, it is possible to manipulate the nanoscale phase separation into hydrophilic and hydrophobic domains [13]. Currently, efforts are being focused on hydrocarbon-based polymers containing sulfonic acid groups on the pendant side chains that can exhibit decent dimensional and thermal stabilities for fuel cell applications [14,15].

Polysulfone (PSf) is an amorphous, high-performance polymer having excellent thermal and chemical stabilities, good resistance to inorganic acids and bases, and outstanding hydrolytic stability against hot water and steam sterilization [16]. Commercially available Udel® polysulfone has been a preferred membrane resin for applications involving water purification and gas separation. Although much effort has been focused on modified polysulfone to suit fuel cell applications [17–20], most of them involve direct sulfonation of the backbone [17] or incorporation of the ionic units via lithiation reaction [18–20], which usually requires harsh reaction conditions such as quite low temperatures and anhydrous, inert atmospheres.

Chloromethylation is a facile and efficient method for introducing functional groups into the polysulfone chains due to the high reactivity of the tethered chloromethyl group (CH_2Cl), which leads to precursors of interest for functional membranes, coatings, ion exchange resins, etc. [21,22]. We present here a convenient synthesis route to prepare new polyelectrolytes with

* Corresponding author. Tel.: +1 512 471 1791; fax: +1 512 471 7681.
E-mail address: rmanth@mail.utexas.edu (A. Manthiram).

0378-7753/$ – see front matter © 2011 Elsevier B.V. All rights reserved.
doi:10.1016/j.jpowsour.2011.05.019

Table 1
Data pertaining to the chloromethylation reaction of polysulfone[a].

Precursor	Time (h)	DC[b]	Yield (%)	M_n[c] (kg mol^{-1})
C-PSf-36	4	0.36	98	36390
C-PSf-44	8	0.44	96	36780
C-PSf-53	12	0.53	95	36980
C-PSf-65	16	0.65	96	37350
C-PSf-86	30	0.86	93	38270
C-PSf-105	44	1.05	91	39010
C-PSf-126	56	1.26	90	39770

[a] Conducted at 50 °C in $CHCl_3$.
[b] Degree of chloromethylation, calculated from the ^{1}H NMR data.
[c] Molecular weight measured in THF at 30 °C.

sulfonated side chains using chloromethylated polysulfones as precursors. The precursors provide the reactive groups (CH_2Cl) for the subsequent nucleophilic substitution reaction to attach the sulfonated side chains. Two types of polyelectrolytes were involved in order to investigate the effect of the side groups with different ionicities (acidic concentration) on the membrane properties. The structural and thermal characterization, proton conductivity, water uptake, and methanol permeability of the synthesized polymers are presented. In addition, electrochemical evaluations of the membrane-electrode assemblies (MEAs) fabricated with these polymer membranes in DMFC are also presented.

2. Experimental

2.1. Materials

Polysulfone (Udel® P-1700, 35 kg mol^{-1}, Solvay Advanced Polymers, USA) was dried under vacuum at 100 °C for 24 h prior to use. 4-hydroxybenzenesulfonic acid sodium salt (99%) and 2-naphthol-6,8-disulfonic acid dipotassium salt (98%) (Acros Organics, USA) were dehydrated by distillation with toluene prior to use. Chloromethyl methyl ether (CMME) (technical grade) and hydrogen peroxide (H_2O_2) solution (30 wt.% in H_2O, ACS reagent) were purchased from Sigma-Aldrich (USA) and used without further purification. Other reagents and materials were used as-received.

2.2. Synthesis of chloromethylated polysulfone (C-PSf-x)

Chloromethylation of polysulfone was performed following a procedure reported elsewhere [21,22]. In a typical reaction, anhydrous zinc chloride (0.221 g) and CMME (3 mL) were added to a solution of polysulfone (4.42 g) in dry chloroform (30 mL) and the resulting mixture was stirred at 50 °C for 4–56 h. The chloromethylated polymer formed was precipitated into methanol, filtered, washed with methanol and de-ionized water several times, and dried at 80 °C under vacuum overnight to give the desired polymers with different degree of chloromethylation (DC). The value of DC was calculated from ^{1}H NMR data as DC = $3A_2/A_1$, where A_1 is the integrated area of the peak corresponding to the isopropylidene moiety (–C(CH_3)$_2$–, six protons), and A_2 is the integrated area of the peak corresponding to the chloromethyl moiety (–CH_2Cl, two protons). These polymers were designated as C-PSf-*x*, where x refers to the value of DC. The data on the chloromethylation reaction are summarized in Table 1.

2.3. Synthesis of sulfonated polysulfone (PSf-sph-y and PSf-sna-z)

The preparation of sulfonated polysulfone was carried out following an optimized procedure available elsewhere [23,24]. The synthesized C-PSf-*x* (10 mmol of CH_2Cl groups), anhydrous K_2CO_3 (2.76 g, 20 mmol), and KI (0.083 g, 0.5 mmol) were added to a solution of 4-hydroxybenzenesulfonic acid sodium salt (3.48 g, 15 mmol) or 2-naphthol-6,8-disulfonic acid dipotassium salt (5.70 g, 15 mmol) in dry dimethylacetamide (DMAc, 100 mL). The resulting mixture was stirred at 100 °C for 48 h, cooled to room temperature, and centrifuged. The resulting liquid was then poured into 2-propanol (200 mL) to precipitate the sulfonated polymer. The precipitate was filtered, washed with excess water three times, and dried under vacuum at 120 °C for 24 h to give the desired polymer with different degrees of substitution (DS). The value of DS was calculated from ^{1}H NMR data similar to the calculation employed for DC. The sulfonated polymers thus obtained by employing 4-hydroxybenzenesulfonic acid sodium salt and 2-naphthol-6,8-disulfonic acid dipotassium salt were designated, respectively, as PSf-sph-*y* or PSf-sna-*z*, where *y* or *z* refers to the value of DS.

2.4. Membrane preparation

The sulfonated polymer in the salt form was dissolved in DMAc to make a 7 wt.% solution. The solution was filtered with a 0.45 μm PTFE filter, followed by casting onto a Petri dish. The cast membrane was dried at 80 °C for 24 h and soaked in de-ionized water to give a transparent and self-standing film with a thickness of 70–80 μm. The membrane was then converted into the acid form by immersing in 2 M H_2SO_4 for 3 days, followed by washing with de-ionized water until the pH value of the washed solution reached a constant value. The fabricated membrane was then kept in de-ionized water.

2.5. Characterization

The ^{1}H NMR (500 MHz) and ^{13}C NMR (126 MHz) spectra were recorded with a Varian Inova 500 spectrometer using $CDCl_3$ or DMSO-d_6 as solvent. Molecular weights were determined by gel permeation chromatography (GPC) with a Waters HPLC system consisting of three Viscotek I-series columns (2 × GMHHRH and 1 × G3000HHR) arranged in series, a 1515 pump, and a 2414 RI detector and are reported relative to polystyrene standards in THF at 30 °C. Differential scanning calorimetry (DSC) analysis was performed with a Mettler Toledo DSC 823[e] from 50 to 300 °C at 10 °C min^{-1} in nitrogen atmosphere. Thermo-gravimetric analysis (TGA) was conducted with a Perkin Elmer 7 system. All the samples were first vacuum dried and kept in the TGA furnace at 150 °C in nitrogen atmosphere for 30 min before recording the TGA plots from 50 to 700 °C at 10 °C min^{-1} in air.

2.6. Ionic exchange capacity (IEC)

The IEC values of the membranes were determined by an acid–base titration. First, the membrane in acid form was immersed in 50 mL 1.0 M NaCl solution for 48 h to replace the protons of the sufonic acid groups with sodium ions. The released protons in the solution were then titrated with 0.1 M NaOH solution using phenolphthalein as an indicator. From the titration data, the IEC (meq. g^{-1}) value was determined as:

$$\mathrm{IEC} = \frac{C \times V}{W} \quad (1)$$

where *C* is the molar concentration of NaOH, *V* is the volume of NaOH consumed, and *W* is weight of the dry membrane.

2.7. Water uptake, swelling ratio, and hydration number

All the samples were first vacuum-dried at 100 °C for 24 h before the experiments. The water uptake (WU) and swelling ratio (SR) were obtained, respectively, from the difference in weight and length of the membranes between the wet to dry states. The sample was immersed in de-ionized water at different temperatures for 24 h and then taken out and wiped with a tissue paper before

the weight and length were measured. The WU and SR values were calculated as:

$$\mathrm{SR}(\%) = \frac{L_{\mathrm{wet}} - L_{\mathrm{dry}}}{L_{\mathrm{dry}}} \times 100\% \quad (2)$$

$$\mathrm{WU}(\%) = \frac{W_{\mathrm{wet}} - W_{\mathrm{dry}}}{W_{\mathrm{dry}}} \times 100\% \quad (3)$$

where W_{wet} and W_{dry} are, respectively, the weight of the wet and dry membranes and L_{wet} and L_{dry} are, respectively, the length of the wet and dry membranes. The hydration number (λ) indicates the number of water molecules absorbed per sulfonic acid groups and is expressed as:

$$\lambda = \frac{\mathrm{WU}}{\mathrm{IEC} \times M_{\mathrm{H_2O}}} \quad (4)$$

where $M_{\mathrm{H_2O}}$ is the molecular weight of water (18.0 g mol^{-1}).

2.8. Oxidative stability

Oxidative stability was measured using the similar method [25]. A small piece of the membrane was soaked in Fenton's reagent (3% H_2O_2 containing 2 ppm $FeSO_4$) at 80 °C. The retained weight (RW) of the membrane after treating with the Fenton's reagent for 1 h and the dissolved time (t) of the membrane into the reagent were used to evaluate the oxidative resistance.

2.9. Proton conductivity

The proton conductivity of the membranes was determined by a two-point probe alternating current impedance spectroscopy using an impedance/gain-phase analyzer (Solartron 1260) and an electrochemical interface (Solartron 1287) over the frequency range of 10–10^6 Hz at different temperatures. The membrane was clamped between two platinum electrodes and immersed into de-ionized water to keep the relative humidity (RH) at 100% during the test. The proton conductivity was calculated as:

$$\sigma = \frac{D}{R \times A} \quad (5)$$

where R, D, and A are, respectively, the resistance, the distance between the two electrodes, and the cross-sectional area of the membrane.

2.10. Methanol permeability

The methanol permeability was measured at room temperature by using a two-chamber glass diffusion cell, which consisted of two identical compartments separated by the test membrane placed on a screw clamp. 10 M methanol solution was placed on one side of the cell and water was placed on the other side. Each chamber was stirred by a magnetic stirrer to ensure uniformity. The concentration of methanol was determined by using Agilent 6850 gas chromatograph. The methanol permeability was calculated as:

$$C_{\mathrm{B}}(t) = \frac{A}{V_{\mathrm{B}}} \frac{\mathrm{DK}}{L} C_{\mathrm{A}}(t - t_0) \quad (6)$$

where A, L, and t are, respectively, the effective area, the thickness of the membrane, and the time, V_{B} is the volume of the diffusion reservoirs, C_{A} and C_{B} are, respectively, the methanol concentration in the feed and diffusion reservoirs, and DK (cm^2 s^{-1}) is the methanol permeability.

2.11. MEA fabrication and electrochemical characterization

The anode and cathode catalyst layers were composed of, respectively, commercial 60 wt.% Pt–Ru (1:1) on Vulcan carbon (Alfa Aesar) and 20 wt.% Pt on Vulcan carbon (Alfa Aesar) with 5 wt.% of Nafion® solution. The catalyst loading in each electrode was 2.0 mg cm^{-2}. For MEA fabrication, the electrodes were prepared by painting the catalyst ink onto a gas diffusion layer (ELAT® LT-1200 W carbon cloth), followed by putting them on both sides of the membrane without hot-pressing. Fuel cell tests were performed at 65 °C using a single-cell hardware (active area of 5 cm^2) fed with 1 M methanol solution at a flow rate of 2.5 mL min^{-1} and humidified oxygen at a flow rate of 200 mL min^{-1} without backpressure. The steady-state fuel cell polarization data were collected after operating the fuel cell for two consecutive days with an intermittent shutdown during the night.

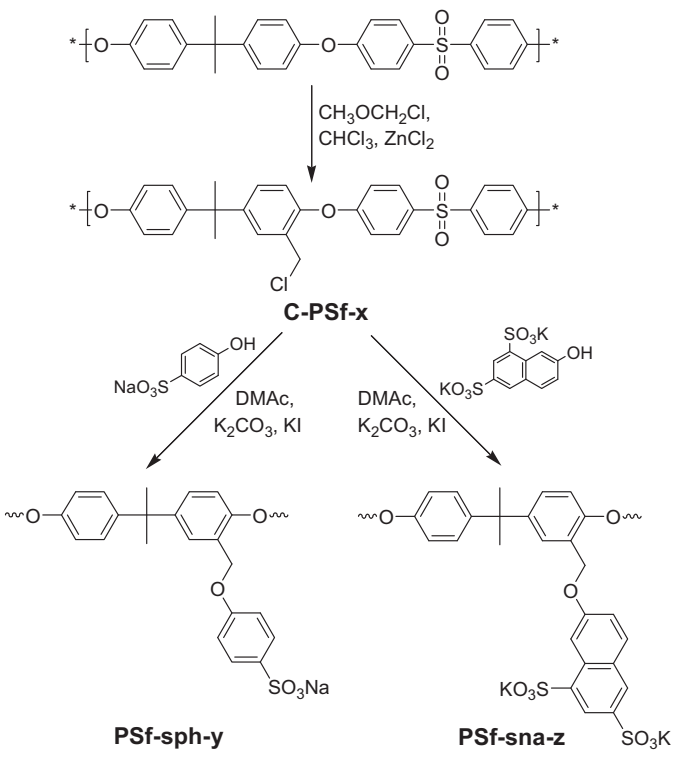

Scheme 1. Preparation of PSf-sph-*y* and PSf-sna-*z* polymers.

Methanol crossover through the membranes was evaluated by a voltammetric method [4]. The measurement was carried out at 65 °C by feeding the methanol solution at a flow rate of 2.5 mL min^{-1} into the anode side of the MEA, while the cathode side was kept under a humidified nitrogen atmosphere. By applying a positive potential at the cathode side, the flux rate of the permeating methanol was determined by measuring the steady-state limiting current density resulting from the electro-oxidation of methanol at the cathode side.

3. Results and discussion

3.1. Polymer synthesis

Two simple steps were involved in the synthesis of polysulfone containing the sulfonated side chains (PSf-sph-*y* and PSf-sna-*z*), as shown in Scheme 1. The first step is the preparation of the precursors (chloromethylated polysulfones) via Friedel–Crafts alkylation reaction, which provides the reactive groups (CH_2Cl) for the subsequent nucleophilic substitution reaction to attach the sulfonated side chains. Therefore, DC determines how many sulfonated groups can be located onto the polymer chains, which in turn determines the degree of sulfonation. The relevance of selected precursors to sulfonated products is shown in Table 2.

Table 2
Thermal properties of sulfonated polymers.

Polymer	Selected precursor	DS[a]	Salt form		Acid form
			T_g (°C)	$T_{d,5\%}$ (°C)[b]	$T_{d,5\%}$ (°C)[b]
PSf-sph-63	C-PSf-65	0.63	198	325	260
PSf-sph-82	C-PSf-86	0.82	213	296	234
PSf-sph-100	C-PSf-105	1.00	257	283	226
PSf-sph-122	C-PSf-126	1.22	281	270	210
PSf-sna-32	C-PSf-36	0.32	209	364	262
PSf-sna-39	C-PSf-44	0.39	221	346	245
PSf-sna-49	C-PSf-53	0.49	247	342	237
PSf-sna-58	C-PSf-65	0.58	278	318	217

[a] Degree of substitution, calculated from the ^{1}H NMR data.
[b] Temperature at which the polymers lose of 5 wt.% in air.

The alkylation reaction was conducted in $CHCl_3$ at 50 °C with $ZnCl_2$ as a catalyst and CMME as the alkalylating agent. We noticed that the chloromethylation of PSf could easily cause gelation, which usually leads to a lower yield of the chloromethylated polymer. In order to improve the chloromethylation without gelation or with less gelation, we studied the parameters that can affect the chloromethylation reaction such as reaction temperature, time, and the amounts of CMME and $ZnCl_2$. After optimization of these parameters, the chloromethylated polysulfone (C-PSf-*x*) with various DC was obtained with high yield (90–98%). Table 1 summarizes the reaction conditions and the results for different batches of the samples. In all cases, the reaction was conducted at 50 °C in $CHCl_3$. The data in Table 1 indicate that the value of DC can be well controlled by adjusting the reaction time while keeping the other parameters constant, which is very important for controlling the incorporation of the sulfonated side chians. Table 1 also gives the molecular weight data for C-PSf-*x*. These data indicate that no significant chain degradation occurs during the chloromethylation reactions. Successful chloromethylation of polysulfone was confirmed by the ^{1}H and ^{13}C NMR spectra. Representative NMR spectra are presented in Figs. 1b and 2a. In Fig. 1b, the new signal at 4.52 ppm was assigned to the protons (denoted as 2 in Fig. 1b) in the CH_2Cl groups, and the other three new peaks (denoted as 3, 4, and 5 in Fig. 1b) were attributed to the protons in the substituted phenyl rings. In Fig. 2a, the signal at 42.4 ppm was assigned to the carbon atoms (denoted as 1 in Fig. 2a) in the CH_2Cl groups.

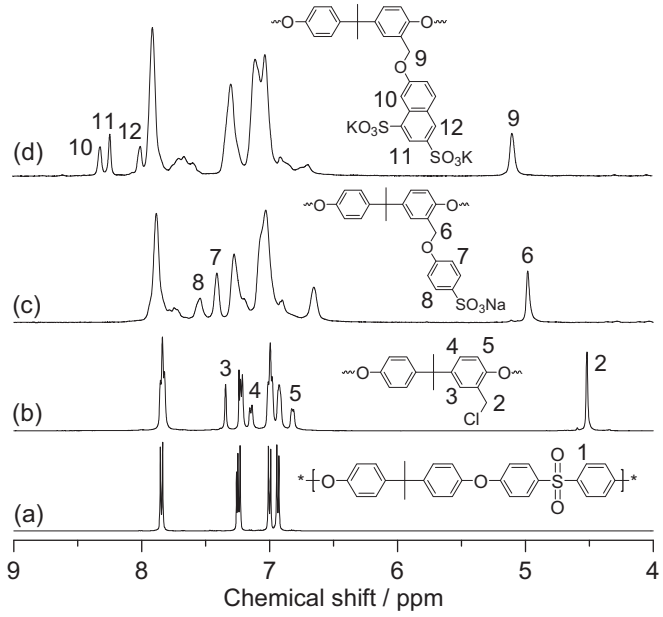

Fig. 1. ^{1}H NMR spectra of PSf, C-PSf-*x*, PSf-sph-*y*, and PSf-sna-*z* polymers.

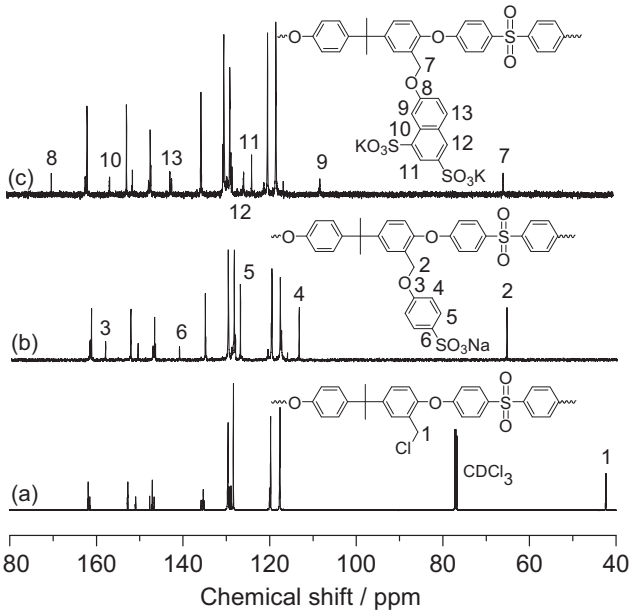

Fig. 2. ^{13}C NMR spectra of C-PSf-*x*, PSf-sph-*y*, and PSf-sna-*z* polymers.

The substitution reaction (the second step) was successfully conducted in DMAc at 100 °C using K_2CO_3 as a base and KI as a catalyst, giving the sulfonated polymers in high yield (90–96%). Incorporation of the sulfonated pendant chains into polysulfone was confirmed by the disappearance of the peak at 4.52 ppm (Fig. 1b) and the appearance of the peak at 4.98 ppm (denoted as 6 in Fig. 1c) or 5.10 ppm (denoted as 9 in Fig. 1d), which was attributed to the protons in ethyoxyl (–CH_2O–) moieties. The incorporation was further confirmed by the ^{13}C NMR spectra, and representative ^{13}C NMR spectra are shown in Fig. 2. The carbon signal of the CH_2Cl groups at 42.4 ppm (Fig. 2a) disappeared, while the signal of the carbon in –CH_2O– moieties was observed at 65.2 ppm (denoted as 2 in Fig. 2b) or at 65.4 ppm (denoted as 7 in Fig. 2c). In addition, some characteristic proton and carbon signals arising from sulfonated side chains were also clearly identified, as seen, respectively, in Figs. 1 and 2.

3.2. Thermal properties

The introduction of sulfonate or sulfonic acid groups increases the intermolecular interactions by pendant ions or hydrogen bonding and molecular bulkiness, which hinders the internal rotation of the high molecular chain segments and leads to increased glass transition temperatures (T_g) for the sulfonated polymers. Table 2 summarizes the T_g values of the sulfonated polymers determined by DSC. No T_g values were detected for the polymers in their acid form at temperatures below their decomposition temperatures (T_d), but glass transitions were observed for their salt forms. As expected, a gradual increase in the T_g values of the salt-form polymers is found with increasing value of DS (Table 2).

The thermal stability of the sulfonated polymers was investigated by TGA. All the samples were pre-heated at 150 °C for 30 min in the TGA furnace to remove moisture. The influence of DS on both T_g and the temperature $T_{d,5\%}$ at which the polymer loses 5 wt.% are summarized in Table 2. While the T_g increases, the $T_{d,5\%}$ decreases with increasing DS value. The data in Table 2 also reveal that all the polymers are stable in air up to 270 °C in the salt form and up to 210 °C in acid form, which is sufficiently high for common fuel cells applications. Fig. 3 shows the TGA curves of the sulfonated polymers in acid form. As seen, all the TGA plots exhibit two

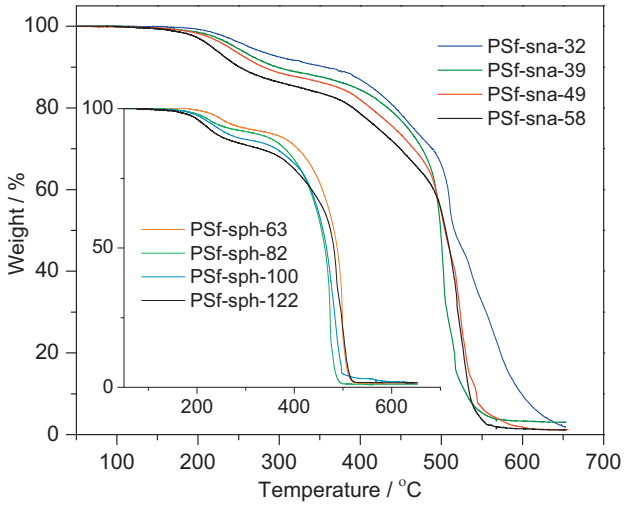

Fig. 3. TGA curves of PSf-sph-*y* and PSf-sna-*z* in acid forms.

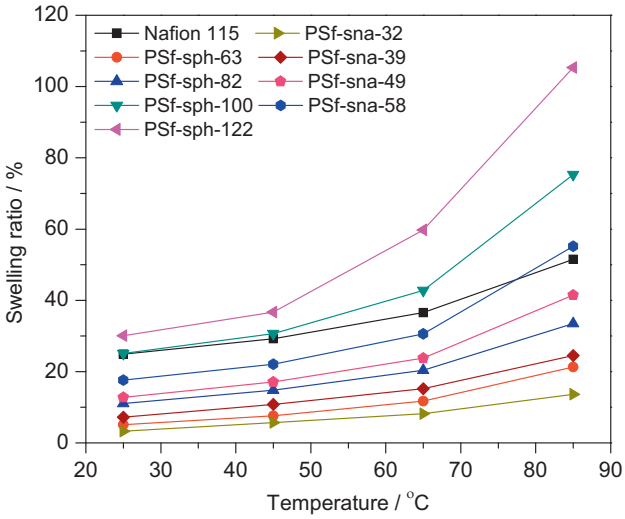

Fig. 5. Swelling ratio of Nafion 115, PSf-sph-*y*, and PSf-sna-*z* in acid forms.

decomposition stages. The first stage around 180–300 °C is possibly associated with the loss of bound water and degradation of the sulfonic acid groups, while the second stage around 380 °C is likely related to the degradation of the side and main chains. As seen in Fig. 3, PSf-sna-*z* exhibit better stability than PSf-sph-*y*, which could be attributed to the lower DS values of PSf-sna-*z*.

3.3. IEC, water uptake, and swelling ratio of the membranes

IEC plays a critical role on determining the proton conductivity of the membranes. The IEC values determined by the acid–base titrations are in the range of 1.10–1.76 meq. g^{-1}, which are in good agreement with the calculated IEC values, as seen in Table 3. Water uptake, known to have a profound effect on membrane properties, is closely related to IEC and can also be expressed as the number of H_2O molecules per sulfonic acid group ($\lambda = [H_2O]/[SO_3H]$). Proper water uptake may lead to suitable swelling ratio and dimensional stability. Fig. 4 shows the water uptake of the membranes as a function of temperature. As expected, the water sorption increases with increasing IEC and temperature. The increase of water uptake with temperature is almost linear up to an IEC value of ~1.4 meq. g^{-1}, but a drastic increase is observed above 65 °C for IEC values >1.50 meq. g^{-1} (Table 3), as seen in Fig. 4. This is referred to as the "percolation threshold". For example, the water uptake increases by 50.7% from 65 to 85 °C for PSf-sph-122, but only by 6.2% for PSf-sph-63 (Table 3). At a given value of IEC, the water uptake of PSf-sph-*y* is higher than that of PSf-sna-*z*, which could be attributed to the higher DS values of PSf-sph-*y*. To reach a similar IEC value, more pendant acid groups need to be incorporated into PSf-sph-*y* backbone compared to that in PSf-sna-*z*, resulting in a higher DS value for PSf-sph-*y*. Obviously, high DS makes PSf-sph-*y* more hydrophilic. In addition, PSf-sna-*z* except PSf-sna-58 show lower water uptake than Nafion 115 from 25 to 85 °C, as seen in Fig. 4.

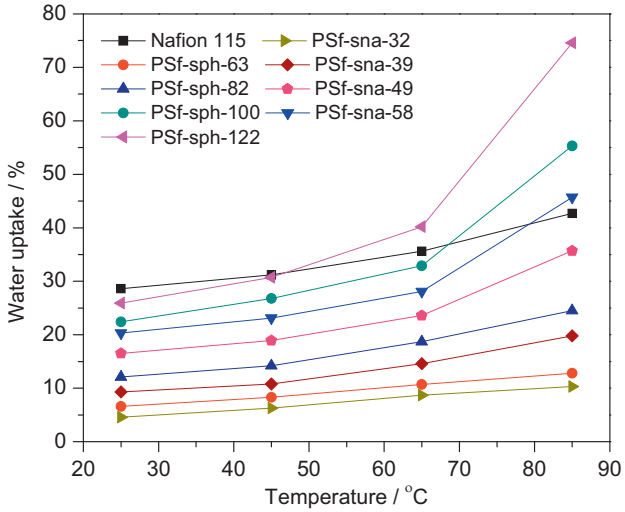

Fig. 4. Water uptake of Nafion 115, PSf-sph-*y*, and PSf-sna-*z* in acid forms.

Fig. 5 shows that the swelling ratio of the membranes also increases with increasing temperature and IEC. At high levels of IEC (>1.50 meq. g^{-1}), the change is significant as the temperature increases. For example, the swelling ratio increases by 74.8% from 65 to 85 °C for PSf-sph-122, but only by 16.2% for PSf-sph-63 (Table 3). At a given value of IEC, the PSf-sna-*z* has a lower swelling ratio than PSf-sph-*y*. For example, the swelling ratio of PSf-sna-49 at 85 °C is 41.5% while that of PSf-sph-100 is 75.2% (Table 3), which might be attributed to the better hydrophilic–hydrophobic separation between the polymer main chain and the sulfonate groups in PSf-sna-*z*. Because of the incorporation of highly ionic groups, the absorption of water can be restricted to a specific hydrophilic domain in the membrane that is molecularly separated from the hydrophobic domain, and the latter domain may retain its cohesion and restrict the swelling [13]. At a given IEC, the DS value of PSf-sna-*z* is much lower than that of PSf-sph-*y*, which can keep the polymer backbone of PSf-sna-*z* more hydrophobic. Meanwhile, the highly ionic groups in PSf-sna-*z* can form better hydrophilic domains. All the membranes except PSf-sph-100 and PSf-sph-122 exhibit a lower swelling ratio than Nafion 115 up to 70 °C, as seen in Fig. 5. Although PSf-sna-58 has lower swelling ratio than Nafion 115 below 70 °C, the swelling ratio of PSf-sna-58 increases sharply above 60 °C, which is attributed to the significant increase in water uptake (Fig. 4.).

3.4. Oxidative stability of the membranes

To evaluate whether PSf-sph-*y* and PSf-sna-*z* can withstand a strong oxidizing environment during the fuel cell operation, the oxidative stability of the membranes was measured as the time required for the samples to start breaking into pieces during immersion in Fenton's reagent at 80 °C and the weight retention after treatment in Fenton's reagent at 80 °C for 1 h. The test results are

Table 3
IEC, water uptake, and swelling ratio of the membranes.

Samples	IEC[a]	IEC[b]	25 °C			85 °C		
			WU[c]	SR[c]	λ[c]	WU	SR	λ
PSf-sph-63	1.18	1.10	6.60	5.13	3.33	12.8	21.3	6.46
PSf-sph-82	1.41	1.33	12.1	11.0	5.05	24.5	33.5	10.2
PSf-sph-100	1.60	1.54	22.4	25.1	8.09	55.3	75.3	19.9
PSf-sph-122	1.81	1.76	25.9	30.2	8.18	76.6	105	24.2
PSf-sna-32	1.15	1.12	4.59	3.30	2.28	10.3	13.7	5.11
PSf-sna-39	1.43	1.32	9.29	7.20	3.91	19.8	24.5	8.33
PSf-sna-49	1.62	1.54	16.5	12.8	5.95	35.7	41.4	12.9
PSf-sna-58	1.76	1.73	20.3	17.6	6.52	45.7	55.2	14.7
Nafion 115	–	0.90	28.6	24.9	17.7	42.7	51.5	26.4

[a] Calculated from the ^{1}H NMR data.
[b] Determined by the acid–base titration.
[c] WU: water uptake (%); SR: swelling ratio (%); λ: hydration number.

given in Table 4. All the membranes have a weight retention of >91% after treatment and did not dissolve within 4 h, suggesting that the membranes show excellent oxidative stability. As seen in Table 4, PSf-sna-*z* exhibit better oxidative stability than PSf-sph-*y*, which is consistent with the thermo-oxidative stability (Fig. 3).

3.5. Proton conductivity and methanol permeability

Proton conductivities of all the hydrated membranes were measured in the temperature range of 25–85 °C under 100% RH and are plotted as a function of temperature in Fig. 6. As seen, the conductivity increases with increasing temperature and IEC. At room temperature, all the membranes except PSf-sph-63 show proton conductivities (Table 4) higher than the threshold value of 10^{-2} S cm^{-1} for practical use in fuel cells. However, as seen in Fig. 6, all the membranes exhibit lower proton conductivities than Nafion 115, which could be attributed to their high activation energies for conduction. Despite a lower water uptake, PSf-sna-*z* shows higher proton conductivity than PSf-sph-*y* (Fig. 6) at low IEC (<1.40 meq. g^{-1}), which might be attributed to the incorporation of highly ionic pendant groups into PSf-sna-*z*. At a similar level of water uptake, highly ionic groups may play a definitive role in determining the proton conductivity since locating highly ionic groups on a short side chain may form a more efficient ionic network when the membranes take up water [13,26]. As we mentioned above, however, water uptake content of PEMs also plays an important role on proton conductivity. At high IEC (>1.50 meq. g^{-1}), PSf-sna-*z* has lower proton conductivity than PSf-sph-*y* (Fig. 6), which might be attributed to the much lower water uptake of PSf-sna-*z* (Fig. 4).

Table 4
Physical properties of the membranes.

Samples	Oxidative stability		σ (S cm^{-1})[c]		DK[d] (×10^{-7} cm^2 s^{-1})
	RW (%)[a]	T (h)[b]	25 °C	85 °C	
PSf-sph-63	98.4	>5	0.008	0.022	2.92
PSf-sph-82	97.5	>5	0.019	0.045	7.41
PSf-sph-100	93.6	>4	0.044	0.089	11.5
PSf-sph-122	91.8	~4	0.065	0.143	14.9
PSf-sna-32	98.7	>5	0.011	0.025	0.36
PSf-sna-39	98.2	>5	0.022	0.051	1.79
PSf-sna-49	97.4	>5	0.041	0.075	3.01
PSf-sna-58	97.1	>5	0.057	0.117	5.23
Nafion 115	98.0	>5	0.090	0.151	16.8

[a] Weights retained after treating the membrane in Fenton's reagent at 80 °C for 1 h.
[b] The time required for the membrane to dissolve in Fenton's reagent at 80 °C.
[c] Measured under 100% relative humidity.
[d] DK: methanol permeability at 25 °C.

Low methanol permeability is critical for practical use of the membranes in DMFC. The methanol permeability of the membranes was measured at room temperature, and the results are given in Table 4. As seen, the methanol permeability increases with increasing IEC and water uptake, indicating that the methanol transport across the membranes is strongly dependent on the water uptake content. As seen in Table 4, PSf-sna-*z* exhibits lower methanol permeability than PSf-sph-*y* and several times lower than Nafion 115 due to the relatively low water uptake and swelling ratio of PSf-sna-*z*. Also, PSf-sph-100 and PSf-sph-122 show high methanol permeability due to their excess water uptake and swelling ratio. Combined with all the other relative properties, PSf-sna-*z* might be a more promising material for DMFC applications.

3.6. Fuel cell performance and methanol crossover

The electrochemical performance and methanol crossover of the MEAs fabricated with the PSf-sna-*z* and Nafion 115 were evaluated in DMFC at 65 °C in 1 M methanol solution, and the results are given in Figs. 7 and 8. It should be noted that both the proton conductivity and methanol crossover have a significant impact on the DMFC performance. It has been reported that membranes having lower methanol crossover exhibit better performances in DMFC compared to Nafion® membrane, which is attributed to a suppressed poisoning and reduced voltage loss at the cathode [27]. Although the proton conductivity of the PSf-sna-58 is lower than

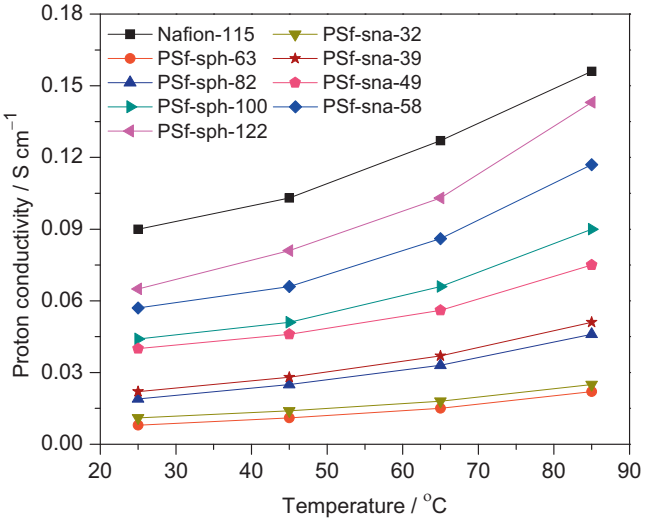

Fig. 6. Proton conductivity of Nafion 115, PSf-sph-*y*, and PSf-sna-*z* in acid forms.

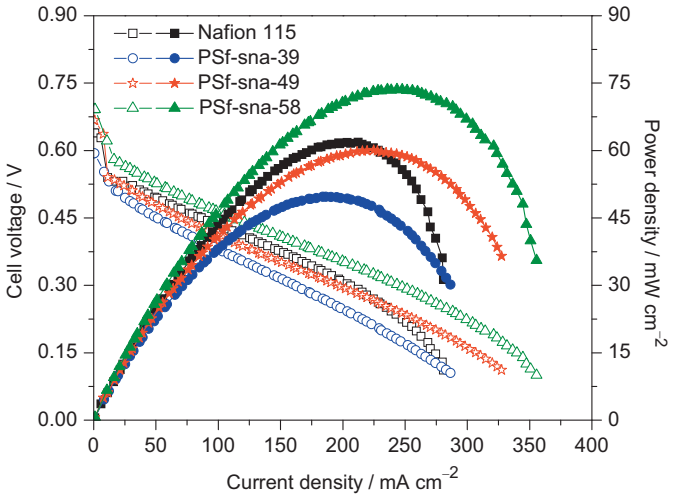

Fig. 7. Polarization curves recorded with the MEAs fabricated with PSf-sna-*z* and Nafion 115 membranes at 65 °C in 1 M methanol.

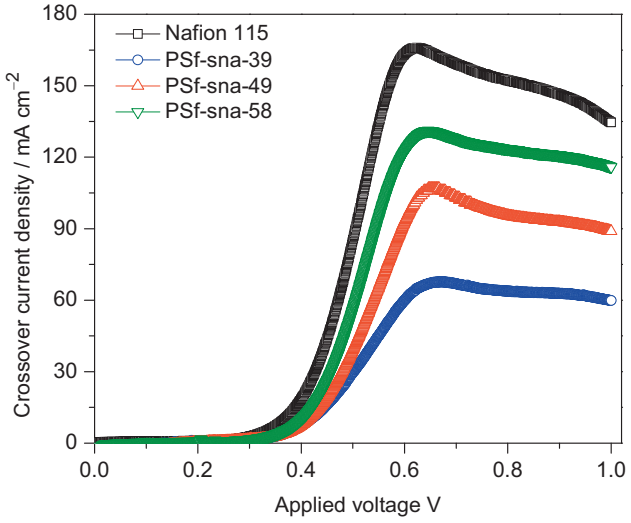

Fig. 8. Methanol crossover current density recorded with the PSf-sna-*z* and Nafion 115 membranes at 65 °C in 1 M methanol.

that of the Nafion 115, the MEA fabricated with PSf-sna-58 exhibits better performance than the MEA fabricated with Nafion 115 as seen in Fig. 7, which is attributed to the good proton conductivity (Fig. 6) and low methanol crossover (Fig. 8) of PSf-sna-58. The open-circuit voltages (OCV) for the PSf-sna-58 membrane (0.69 V) is higher than that of Nafion 115 membrane (0.63 V), and the maximum powder density of the PSf-sna-58 membrane (73.6 mW cm^{-2}) is 1.2 times higher than that of the Nafion 115 (61.8 mW cm^{-2}). Although the MEA fabricated with PSf-sna-39 has the lowest methanol crossover, it shows the worst electrochemical performance (Fig. 7), which is attributed to the high membrane resistance arising from the inferior proton conductivity of PSf-sna-39 (Fig. 6).

4. Conclusions

Two series of polysulfone-based ionomers with sulfonic acid groups in the side chains have been synthesized by a facile two-step process and characterized. The degree of sulfonation could be easily adjusted by controlling the degree of chloromethylation in the first step. Optimized polymer compositions such as PSf-sna-58 exhibit better performance in DMFC compared to Nafion 115 membrane despite lower proton conductivity because of lower methanol crossover. The various advantages associated with PSf-sna-58 such as low cost, high thermal and oxidative stabilities, low water uptake, and low methanol permeability make it an attractive alternate for DMFC. The study demonstrates that ionomers based on pendant sulfonic acid groups offer a promising approach for developing high-performance membranes for DMFC.

Acknowledgements

Financial support by the Office of Naval Research MURI grant number N00014-07-1-0758 is gratefully acknowledged.

References

[1] J.P. Shoesmith, R.D. Collins, M.J. Oakley, D.K. Stevenson, J. Power Sources 49 (1994) 129–142.
[2] M. Rikukawa, K. Sanui, Prog. Polym. Sci. 25 (2000) 1463–1502.
[3] K.D. Kreuer, J. Membr. Sci. 185 (2001) 29–39.
[4] X. Ren, T.E. Springer, S. Gottesfeld, J. Electrochem. Soc. 147 (2000) 92–98.
[5] B. Bae, H.Y. Ha, D. Kim, J. Membr. Sci. 276 (2006) 51–58.
[6] L. Li, J. Zhang, W. Wang, J. Membr. Sci. 226 (2003) 159–167.
[7] Y.-Z. Fu, A. Manthiram, M.D. Guiver, Electrochem. Commun. 9 (2007) 905–910.
[8] H. Kim, H. Chang, J. Membr. Sci. 288 (2007) 188–194.
[9] Y.-M. Sun, T.-C. Wu, H.-C. Lee, G.-B. Jung, M.D. Guiver, Y. Gao, Y.-L. Liu, J.-Y. Lai, J. Membr. Sci. 265 (2005) 108–114.
[10] J.K. Lee, W. Li, A. Manthiram, J. Membr. Sci. 330 (2009) 73–79.
[11] F. Zhai, X. Guo, J. Fang, H. Xu, J. Membr. Sci. 296 (2007) 102–109.
[12] M.A. Hickner, H. Ghassemi, Y.S. Kim, B.R. Einsla, J.E. McGrath, Chem. Rev. 104 (2004) 4587–4612.
[13] T.B. Norsten, M.D. Guiver, J. Murphy, T. Astill, T. Navessin, S. Holdcroft, B.L. Frankamp, V.M. Rotello, J. Ding, Adv. Funct. Mater. 16 (2006) 1814–1822.
[14] Z. Hu, Y. Yin, S. Chen, O. Yamada, K. Tanaka, H. Kita, K. Okamoto, J. Polym. Sci., Part A: Polym. Chem. 44 (2006) 2862–2872.
[15] B. Lafitte, P. Jannasch, Adv. Funct. Mater. 17 (2007) 2823–2834.
[16] T.E. Bugel, Polysulfone: A New Engineering Thermoplastic, ASM, Materials Park, 1965.
[17] R. Nolte, K. Ledjeff, M. Bauer, R. Mülhaupt, J. Membr. Sci. 83 (1993) 211–220.
[18] J. Kerres, W. Cui, S. Reichle, J. Polm. Sci. Part A: Polym. Chem. 34 (1996) 2421–2438.
[19] B. Lafitte, L.E. Karlsson, P. Jannasch, Macromol. Rapid Commun. 23 (2002) 896–900.
[20] B. Lafitte, M. Puchner, P. Jannasch, Macromol. Rapid Commun. 26 (2005) 1464–1468.
[21] A. Warshawsky, N. Kahana, A. Deshe, H.E. Gottlieb, R. Arad-Yellin, J. Polym. Sci. Part A, Polym. Chem. 28 (1990) 2885–2905.
[22] E. Avram, M.A. Brebu, A. Warshawsky, C. Vasile, Polym. Degrad. Stabil. 69 (2000) 175–181.
[23] K.M. Brinner, J.M. Kim, H. Habashita, I.Y. Gluzman, D.E. Goldberg, J.A. Ellman, Bioorg. Med. Chem. 10 (2002) 3649–3661.
[24] E.S. Lee, S.K. Hong, Y.S. Kim, J.H. Lee, J.C. Won, J. Appl. Polym. Sci. 109 (2008) 1–8.
[25] B. Liu, G.P. Robertson, D.-S. Kim, X. Sun, Z. Jiang, M.D. Guiver, Polymer 51 (2010) 403–413.
[26] Z.Q. Shi, S. Holdcraft, Macromolecules 38 (2005) 4193–4201.
[27] M.H. Yildirim, D. Stamatialis, M. Wessling, J. Membr. Sci. 294 (2008) 364–372.